Reference-Point Algorithms for Active Motion Compensation of Towed Bodies

Clark Calnan, Robert J. Bauer
Dalhousie University
Department of Mechanical Engineering
Halifax, NS, Canada
cl213898@Dal.ca; Rober.Bauer@Dal.ca

Rishad A. Irani
Carleton University
Department of Mechanical and Aerospace Engineering
Ottawa, ON, Canada
Rishad.Irani@Carleton.ca

***Abstract*—Active heave compensation systems are typically single degree-of-freedom systems which operate vertically to attenuate the vertical effects of wave motion. To apply compensation to towed bodies – which experience significant multiple-degree-of-freedom disturbances – a generalized motion compensation system using a "reference-point algorithm" is required which determines the length of tow cable that should be reeled in or reeled out by an on-board winch system in response to external wave motion. This paper proposes, implements, and assesses four different reference-point algorithm approaches in both experimental and simulated environments. Of the proposed reference-point algorithms, the method which directly accounts for the towline angle proved to be most effective in both simulation and experimentation. It was found that there was little improvement between real-time measurements of the towline angle and an assumed constant nominal towline angle – indicating a potential cost saving opportunity through the reduction of real-time sheave-angle measurement.**

Keywords — Towed body, Heave Compensation, Motion Compensation, Active Heave Compensation.

Preprint

I. Introduction and Problem Definition

While at sea, a ship on the ocean surface is subjected to waves which impose disturbance motions on the ship. The resulting ship motion can be described in terms of ship displacements about the vessel's centre of gravity (CG) in six degrees-of-freedom, namely heave, surge, sway, roll, pitch, and yaw. If the surface ship is towing a submerged body containing oceanographic equipment, then any ship motion or perturbations at the water surface can impart disturbances on the submerged towed body via the tow tether. A motion compensation method is, therefore, needed to effectively attenuate unwanted towed-body motion caused by wave motion at the surface. Motion compensation research tends to focus on vertical heave compensation [1]. Some of the most common applications of vertical heave motion compensation are for offshore drill operation and to stabilize Remotely Operated Vehicles (ROVs). In these scenarios, vertical heave tends to be the most dominant disturbance acting on the system and the tow cable is primarily oriented in the vertical direction resulting in a one-degree-of-freedom compensation system. Thus, as the surface vessel heaves up, the winch

must let out line equal to the heave displacement to compensate for the unwanted motion. Similarly, as the surface vessel lowers, the winch must reel line in equal to the displacement.

As the name suggests “towed bodies” operate when their host ship is underway and, as waves interact with the surface vessel, the tow point or overboarding sheave is not limited to simple vertical heave motion. Furthermore, the towline exits from the sheave tow point at an angle θ. Fig. 1 shows a schematic of a hypothetical ship and its towed body experiencing perturbations from wave motion, where the cable connecting the towed body to the active motion compensation winch passes over a sheave mounted at the surface vessel’s stern. In the case of a purely vertical heave compensation system, the sheave angle θ depicted in Fig. 1 is equal to zero and determining the amount of cable which needs to be reeled in or out is straightforward if one knows the vertical motion of the vessel. In the case of towed bodies, however, the sheave angle θ is non-zero and the amount of cable which needs to be reeled in or out is not as obvious.

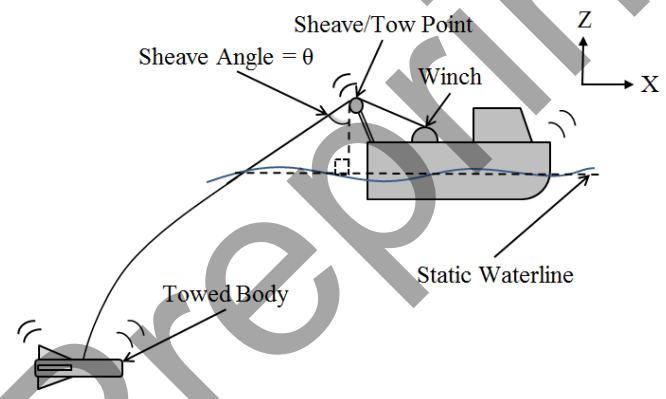

Fig. 1: Schematic of a research vessel transferring motion to a towed body via its tether. The towline passes over the vessel’s sheave before crossing the waterline and is attached to the underwater towed body

Much of the literature pertaining to towed-body and tow-cable motion and simulation is concerned with describing the spatial configuration of the towed system in order to predict towed-body motion during a host vessel maneuver. Yang *et al.* [2], for example, develop a three-dimensional lumped-mass cable model which includes consideration for bending and torsional effects. Yang *et al.*’s [2] cable model is used to simulate the behaviour of a towed array during circular host vessel manoeuvers. Kamman and Huston [3] neglect cable torsion, but extend the formulation of a multi-body cable model to include cable-link contraction and extension to capture the effects of a tow cable being reeled in or out. Also in their work, Kamman and Huston [3] present the simulated spatial configuration of a towed system for a starboard turn manoeuver. Cable bending and torsion are also neglected in the cable model

Preprint

presented in Wang *et al.* [4]. The Wang *et al.* cable model is used to simulate multiple towed systems used for spatial positioning of a seismic acoustic system exposed to both uniform and non-uniform current conditions.

Many researchers have used lumped-element models to simulate cable behaviour. For example, Lambert *et al.* [5] developed a lumped-mass cable model formulation which was solved using a Runge-Kutta integrator for the DOLPHIN semi-submersible towing vehicle which pulled the AURORA Towfish. Their work pertained to the optimization of the system's design and operation. Driscoll and Nahon [6] also developed a lumped-mass cable model for an ocean mooring. Their system was solved using a fourth-fifth order Runge-Kutta technique with an adaptive step size. Sun *et al.* [7] used a lumped-mass cable model to examine directional stability, maneuverability, safety and control characteristics of a towed body. Park *et al.* [8] used a low-tension cable system with a rotational stiffness to describe the cable.

While a winch can be used to reel in and reel out tow cable, the present authors could not find any published liturature that explains, for a known generalized ship motion, how much cable should be reeled in or out by the winch controller for towed-body active motion compensation systems. To help extend current motion compensation and modelling efforts, this paper builds upon the previous two-dimensional analyses of the current authors [9] and investigates four different reference-point compensation strategies that use a winch controller to try to effectively decouple ship motion from a towed body.

Fig. 2 depicts the proposed control loop where on-board measurements of ship perturbations with an Inertial Measurement Unit (IMU) as well as a sheave angle measurement system can be implemented into an active motion compensation control architecture to provide a reference point for a closed-loop controller. Ship motion consisting of roll, pitch, yaw, surge, and heave, with knowledge of the ship geometry, can be used to determine the planar displacement of the host vessel sheave in global *x*- (surge) and *z*- (heave) directions as depicted in Fig. 1. The sheave motion, in conjunction with the sheave angle θ, may be used by the reference-point algorithms to compute a suitable length of cable to reel in or reel out in response to wave effects.

Preprint

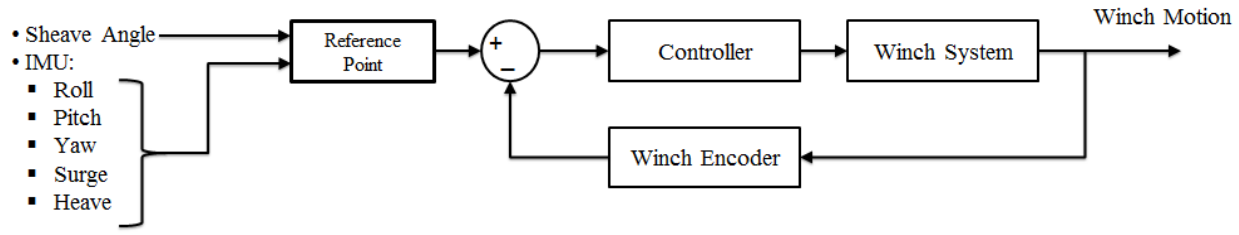

Fig. 2: Proposed control loop using on-board IMU and sheave angle to provide a reference tracking signal for the closed-loop winch control system

The following section introduces the four different reference-point compensation strategies being proposed to determine the winch controller's reference tracking signal. Section III describes experimental tests which were conducted to compare the

performance of the various reference-point algorithms. Section IV describes the 3D computer simulator which was developed to evaluate the performance of the reference-point algorithms over a range of operating conditions, while Sections V and VI discuss this study's results and conclusions, respectively.

II. Reference-Point Algorithms

The four proposed reference-point motion compensation approaches developed by the present authors are referred to as:

1. Simplified Waterline Algorithm
2. Rigorous Waterline Algorithm
3. Simplified Sheave Algorithm
4. Rigorous Sheave Algorithm

The approaches were developed by assuming that the only sensors available are an IMU on the surface vessel to measure the ship's roll, pitch, yaw, surge, heave, and sway, a winch encoder to measure the length of cable that has been reeled in or out, and a tow-angle sensor to measure the angle of the towline as it leaves the sheave to enter the water. While it is possible to equip the towed body with an IMU to report its location underwater for additional controller feedback, this towed-body motion information is generally not available nor always feasible to acquire.

Fig. 3 illustrates the different sheave and waterline methods proposed in this paper to determine the amount of cable the winch motor should reel in or out for active motion compensation. The upper diagram in Fig. 3 depicts what the present authors call the "Waterline" algorithm. The Waterline method attempts to compensate for unwanted towed-body motion by ensuring that the same point along the cable always enters the water. A control action is carried out by providing a reference signal to the control loop illustrated in Fig. 2 equivalent to the difference between C and C_{Nom}, as depicted in Fig. 3. The lower diagram in Fig. 3 illustrates what the present authors call the "Sheave" algorithm, which determines the appropriate reference signal based on the displacement of the vessel's sheave tow point projected along the tow cable. The Sheave and Waterline methods can be implemented with real-time knowledge of the actual sheave angle (referred to in this paper as "Rigorous Waterline" and "Rigorous Sheave") or without real-time knowledge of the actual sheave angle where a nominal sheave angle is used and assumed to be constant (referred to as "Simplified Waterline" and "Simplified Sheave"). Simplified algorithms, therefore, do not require a tow-angle sensor. Rigorous and Simplified versions of the Sheave and Waterline algorithms constitute the four reference-point approaches for the towed-body motion compensation explored in this paper.

Preprint

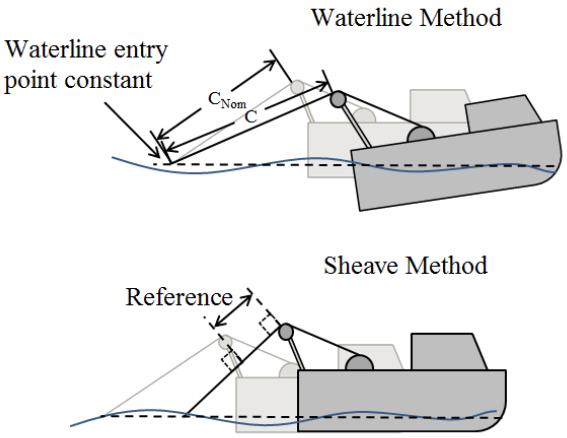

Fig. 3: TOP: Schematic of the "Waterline" methods, which maintains a constant waterline entry point relative to the host vessel's desired forward trajectory; BOTTOM: Schematic of the "Sheave" methods, which determine the desired cable adjustment based on the motion of the vessel's sheave projected along the tow cable.

A. Waterline Methods

The Simplified Waterline method is depicted in the upper diagram in Fig. 4. With this compensation method, the vertical motion of the vessel's sheave can be calculated from IMU data; however, since the actual sheave angle θ is unknown, the actual exposed tow cable length cannot be completely determined. For this case, a nominal constant sheave angle θ_{Nom} is used to compute the amount of tow cable exposed above the waterline. The lower diagram in Fig. 4 illustrates the Rigorous Waterline algorithm, in which the actual sheave angle θ is measured in real-time. In this case, both the sheave height above the static waterline and sheave angle are known, which enables the exposed line length to be fully defined and used by the winch controller to ensure that the same point along the cable enters the water.

Preprint

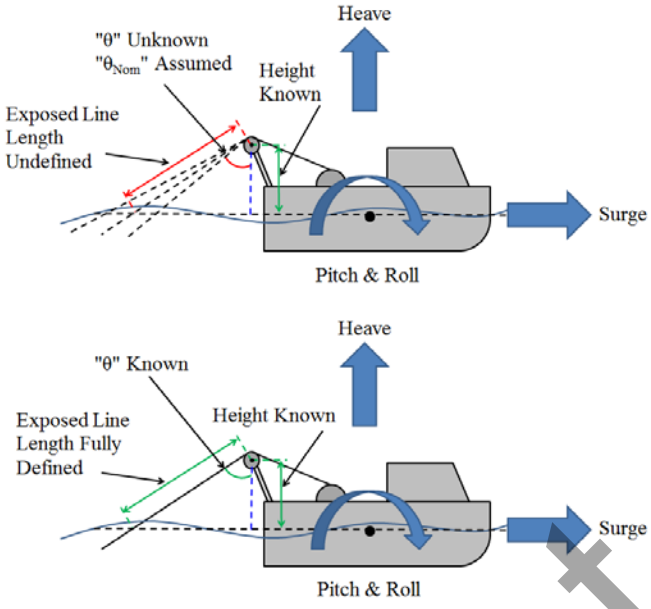

Fig. 4: TOP: Schematic of the "Simplified Waterline" algorithm and the approximate value for exposed line length; BOTTOM: Schematic of the "Rigorous Waterline" and the more accurate calculation of exposed line length.

Equations (1) and (2) describe the calculation of the reference value for both Simplified Waterline and Rigorous Waterline algorithms, respectively. R indicates the reference value for the control loop, H indicates the sheave height above the static waterline measured from the ship's IMU, and H_{nom} indicates the nominal height of the centre of the sheave above the static waterline.

$$R_{Simplified\ Waterline} = \frac{H}{\cos\theta_{nom}} - \frac{H_{nom}}{\cos\theta_{nom}} = \frac{H - H_{nom}}{\cos\theta_{nom}} \quad (1)$$

$$R_{Rigorous\ Waterline} = \frac{H}{\cos\theta} - \frac{H_{nom}}{\cos\theta_{nom}} \quad (2)$$

B. Sheave Methods

Fig. 5 depicts the Simplified Sheave algorithm where the effects of the surface vessel sheave's motion can be calculated. For this case, the sheave angle θ is unknown; therefore, a nominal constant sheave angle θ_{Nom} is assumed. The resulting displacement of the sheave tow point in the x and z directions measured relative to the nominal undisturbed position of the sheave (indicated with Δx and

Preprint

Δz in Fig. 5) can then be projected along the tow cable entering the water at the nominal angle θ_{Nom} to determine the amount of cable that needs to be reeled in or out by the winch controller.

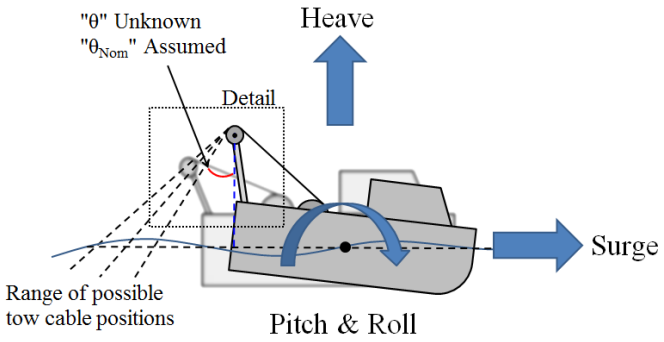

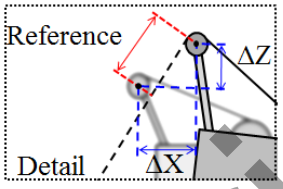

Fig. 5: TOP: Schematic of the "Simplified Sheave" algorithm with a range of possible sheave angles; BOTTOM: Detail view of the sheave and the nominal sheave angle.

Fig. 6 illustrates the Rigorous Sheave algorithm in which, similar to the Rigorous Waterline algorithm, the sheave angle is measured in real-time. As a result, the displacement of the sheave tow point can be projected onto the actual tow cable to determine the reference that the winch controller needs to track.

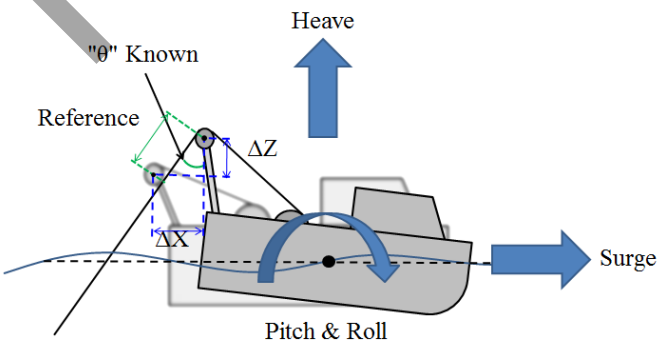

Fig. 6: Schematic of the "Rigorous Sheave" algorithm.

The calculation of the reference value for both Simplified Waterline and Rigorous Waterline algorithms are calculated as follows:

Preprint

$$R_{Simplified\ Sheave} = \Delta x \sin\theta_{nom} + \Delta z \cos\theta_{nom} \quad (3)$$

$$R_{Rigorous\ Sheave} = \Delta x \sin\theta + \Delta z \cos\theta \quad (4)$$

where R indicates the reference value, Δx and Δz represent the current displacement of the host vessel sheave projected onto the global x and z axes, and θ and θ_{nom} indicate the sheave angle and nominal sheave angle, respectively.

C. Method Implimentaiton and Intial Comparision

To illustrate the different results obtained by the four reference-point algorithms, an example scenario is presented in Table 1 consisting of a nominal and actual sheave-angle value along with disturbance and offset values for the host vessel sheave tow point. The values in Table 1 indicate that the host vessel sheave has surged forward 0.5 m along the x axis and heaved upward 0.5 m along the z axis in excess of the expected steady-state position. As a result, the sheave is 2 m above the static waterline. Additionally, the nominal sheave angle of 1 rad (57.3°) is assumed to be incorrect, with the actual sheave angle being 0.95 rad (54.4°). The resulting reference signals for each of the reference algorithms are also presented. It is interesting to note that, for this example, there is a 40% difference between the reference signals of the waterline methods, while there is only a 1% difference between the reference signals of the sheave methods.

TABLE 1: EXAMPLE PARAMETERS AND CORRESPONDING ALGORITHM REFERENCE VALUES

Parameter	Value	Units
X disturbance	0.5	m
Z disturbance	0.5	m
Z offset	2	m
Nominal Sheave Angle	1	rad
Actual Sheave Angle	0.95	rad
$R_{Simplified\ Waterline}$	0.925	m
$R_{Rigorous\ Waterline}$	0.662	m
$R_{Simplified\ Sheave}$	0.691	m
$R_{Rigorous\ Sheave}$	0.698	M

Preprint

III. Flume Tank Experiments

To test the performance of the four proposed reference-point algorithms, a small-scale test apparatus was developed and used in a recirculating flume water tank, as shown in Fig. 7. This flume-scale apparatus was designed using rack and pinion mechanisms to produce repeatable tow-point motion. The resulting test rig had a maximum heave motion (*z*-axis motion), maximum sway motion (*y*-axis motion), and maximum horizontal motion (*x*-axis surge) of ±4 cm. A small winch was attached to the actuated platform with a 101 cm length of 0.045 mm nylon line spooled around it to act as a tow cable. To measure the sheave angle, a balanced cable follower with a non-contact absolute encoder was mounted beside the winch. The sheave angle measurement was used for controller feedback in the Rigorous Waterline and Rigorous Sheave reference-point algorithms. A spherical towed body was used so that a simple and classical solution could be benchmarked without the additional complexities associated with tow-body dynamics arising from more complex shapes. A spherical towed body is also used by Kamman and Huston [3] in their work with towed systems.

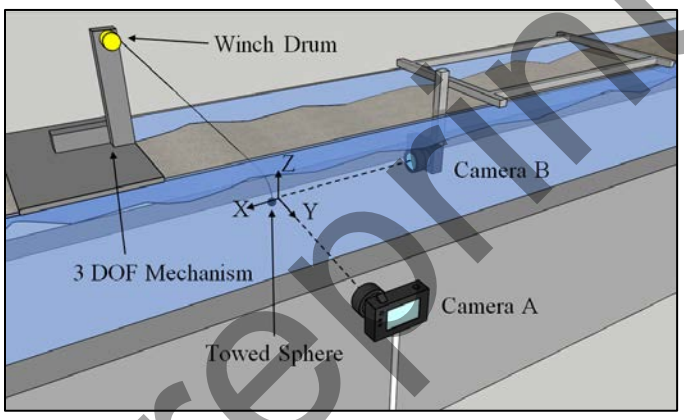

Fig. 7: Diagram of the flume-scale test apparatus

The flume-scale test apparatus was mounted above a recirculating flume tank as shown in Fig. 7 and the flow profile of the flume tank was measured using a Vectrino Doppler velocimeter [10]. Fluid flow velocity near the towed body was found to be 0.33 m/s.

The size of the towed body and length of tow cable used in the flume-scale test apparatus shown in Fig. 7 were determined based on Froude number relationships between a full-scale towed system described in Sun *et al.* [7] and the flume-scale test apparatus. This non-dimensional approach is described in Quan *et al.* [11] and used for their heave compensation work, where the equivalences indicated by Equations (5) and (6) must be maintained for dimensional similarity. The Froude criterion is described by:

Preprint

$$\frac{\lambda_v^2}{\lambda_g \lambda_l} = 1 \tag{5}$$

where λ indicates a ratio of the full-scale system parameters to the flume-scale model parameters, such that λ_v is the velocity ratio of the flow, λ_g is the ratio of gravitational fields, and λ_l is the ratio of characteristic lengths. Full-scale system parameters were borrowed from Sun *et al.* [7], Walton and Brillhard [12], as well as an Australian Defence Science and Technology Organisation (DSTO) report [13]. Quan *et al.* [11] used cable length as the characteristic length to emulate the catenary and cable dynamics and the present authors followed the same approach. The non-dimensional analysis is further constrained by:

$$\frac{\lambda_m}{\lambda_\rho \lambda_l^3} = 1 \tag{6}$$

where λ_ρ is the ratio of fluid densities and λ_m is the ratio of effective towed mass composed of the towed-body mass and partial tow cable mass as derived in [11]. Froude number relationships are listed in Table 2. Using the values from Table 2 in Equations (5) and (6) yields:

$$\frac{\lambda_m}{\lambda_\rho \lambda_l^3} = \frac{2631190}{123.8^3} = 1.39 \cong 1 \tag{7}$$

$$\frac{\lambda_v^2}{\lambda_g \lambda_l} = \frac{11.1^2}{123.8} = 0.99 \cong 1 \tag{8}$$

It should be noted that while 1.39 in Equation (7) might not appear to be approximately equivalent to 1 as in Equation (6), perfect equivalence to 1 in Equation (7) would correspond to a full-scale tow cable length of 138 m, which is only about 10% longer than the full-scale length of 125 m due to the cubed relationship. From the approximate equivalences observed in Equations (7) and (8), the Froude criterion is considered to be upheld within the context of this research to evaluate the various reference-point algorithms.

The corresponding flume-scale test apparatus parameters are presented in Table 3.

Preprint

TABLE 3: TEST APPARATUS PARAMETERS

Parameter	Value	Units
Vertical sheave offset	46	cm
Horizontal sheave offset	72	cm
Towline diameter	0.45	mm
Towline mass per length	0.20	g/m
Towed sphere diameter	10	mm
Towed sphere mass	1.33	g
Nominal submerged towline	35	cm

Ship motion data was digitized from the Australian DSTO report [13]. The data was then resolved into three translational degrees-of-freedom for a towed-body winch located at the ship's stern. This motion was scaled down to allow for appropriate motion of the flume-scale mechanism within its 4×4×4 cm^3 motion envelope. The resulting *x*, *y*, and z motion of the sheave tow point is shown in Fig. 8. For each trial, the test apparatus' actuators tracked the scaled motion path.

Preprint

TABLE 2: FLUME-SCALE AND FULL-SCALE TOWED SYSTEM PARAMETERS.

Parameter	Full-Scale System	Flume-Scale Apparatus	Λ
Towline length	125 m	1.01 m	$\lambda_l = 123.8$
Relative flow velocity	3.66 m/s	0.33 m/s	$\lambda_v = 11.1$
Effective towed mass	3684 kg	0.00140 kg	$\lambda_m = 2631190$
Gravity field	9.81 m/s^2	9.81 m/s^2	$\lambda_g = 1$
Seawater density	1026 kg/m^3	1026 kg/m^3	$\lambda_\rho = 1$

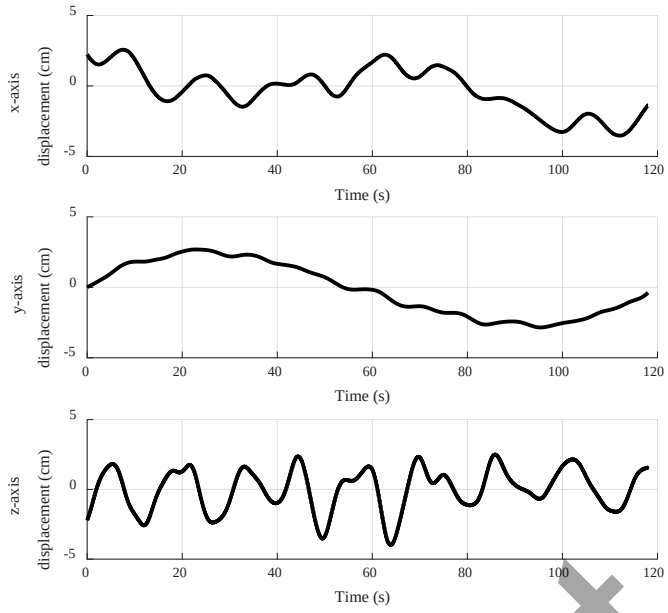

Fig. 8: Vertical and horizontal motion of the flume-scale sheave tow point

Motion of the towed body was captured by a digital camera positioned beside the flume tank's acrylic wall and another underwater camera positioned in line with the flume tank flow behind the towed sphere. The video footage was decomposed into image frames and image analysis was carried out to track and record the towed-body motion over time. Five image frames per second were used to describe the towed-body motion, resulting in a motion trace of 590 data points for each trial.

To test the four different reference-point compensation methodologies, a PD controller was designed to control the winch on the experimental apparatus, while a National Instruments MyRIO controller was used to execute the compensation methodologies at a rate of 1 kHz. The controller gains were tuned to a 90% rise time of 0.12s. The controller output is provided as a PWM signal ranging from 0 to 1, while the winch system output was measured in encoder counts with a resolution of 720 counts per revolution.

IV. Towed System Model

The lumped-mass cable model developed for this research was constructed with Matlab's SimMechanics toolbox using a series of SimMechanics rigid-body elements – a modelling and simulation approach which has previously proven effective for the present authors [14]. Universal joints were used between each body element where stiffness and damping forces were applied, similar to the work of Park *et al.* [8]. The resulting system was solved using Simulink's common and robust ode45 solver.

Preprint

Building on the work of previous lumped mass cable models [2-5], the drag force $F_{D,i}$ on each cable element i was calculated along the element reference axes x_i, y_i and z_i as:

$$F_{D,i} = \frac{1}{2}\rho_w C_D A_E |U_i| U_i \tag{9}$$

where ρ_w is the density of the water, A_E is the projected area of the cable along the element reference axis, C_D is the drag coefficient associated with that projected geometry, and U_i is the relative velocity between the cable link and the fluid flow in the x_i, y_i and z_i directions. The net body forces of the cable weight and buoyancy were also added to each link.

The cable model was connected to the towing sheave via a one-dimensional prismatic joint within SimMechanics with a universal joint at the tow point. This joint mimicked the cable being reeled in or out by the winch following one of the four compensation methodologies under investigation.

A. Flume-scale simulator

The flume-scale towed system represents a low-tension application where rotational strain is dominant. As a result, the 0.045 mm nylon tow cable's rotational stiffness and damping values were identified by observing the impulse response of a length of cable and fitting the resulting response frequency and logarithmic decrement rate to a simple second-order mass-stiffness-damper model. These dynamic parameters, in addition to other simulator parameters are summarized in Table 4.

TABLE 4: SIMULATION TOWLINE PARAMETERS

Parameter	**Value**	**Units**
Young's modulus of towline	3	GPa
Towline density	1221	kg/m^3
Rotational stiffness	4.488×10^{-6}	Nm/deg
Rotational damping	3.116×10^{-9}	Nms/deg

The fluid velocity profile and turbulence which were measured in the flume tank experiment were replicated in simulation and applied to each of the submerged towed system elements. To simulate the effect of turbulence, a white-noise signal was generated and then filtered using a low-pass filter to capture the frequency components detected with the Vectrino velocimeter. The signal was then scaled such that its variance was consistent with measurements taken with the Vectrino velocimeter. The resulting signal was then superimposed onto the flow in the *x*, *y*, and *z* directions within the simulator. The flume-scale winch dynamics were also

Preprint

identified and incorporated into the flume-scale simulator. This process is described in greater detail in the authors' previous work [15].

To validate the flume-scale simulator, the simulation and experimental results were compared for the stationary tow-point mechanism case. Fig. 9 compares the flume-scale simulation and experimental results for this stationary mechanism case with the sheave tow point and flume-tank waterline superimposed for scale. The origin for this plot is taken as the centre of the field of view of the experimental test setup's digital cameras. Fig 9 highlights that there is reasonable agreement between the experimental and simulation results. The centroids of both towed-sphere traces differ by 1.2 cm which is a relatively small level of error given that this difference corresponds to only 1.2% of the total tow-cable length. The relatively small deviations in the results are attributed to un-modelled complex turbulent and fluid phenomena. While a coupled MATLAB Control System and Computational Fluid Dynamic (CFD) simulation could potentially improve the correlation between the experimental and simulation results, the computational power required for this type of analysis is very high. Thus, in the context of the current study, the SimMechanics model was deemed appropriate for the control-system development and investigation.

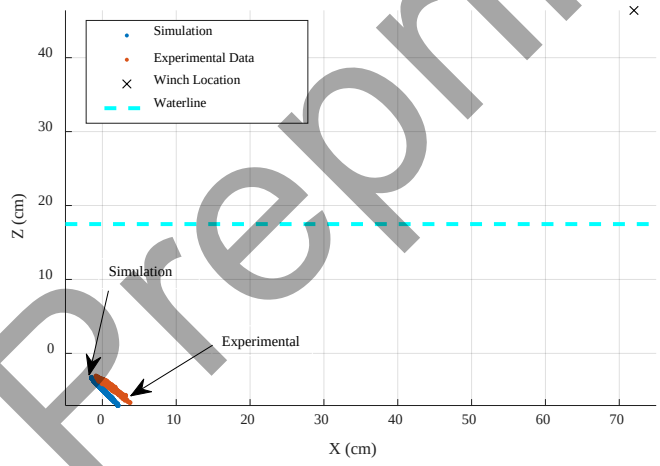

Fig. 9: Superposition of experimental and simulator results for a stationary tow-point mechanism test

B. *Full-scale simulator*

Full-scale simulator parameters were selected to reflect an FFG7 vessel from the Australian DSTO report [13] towing a spherical towed body which is 0.9 metres in diameter. Towed-body properties were consistent with frontal area and volume described in Walton and Brillhard [12]. The key simulator parameters are presented in Table 5.

Preprint

TABLE 5: FULL-SCALE SYSTEM TOW PARAMETERS

Parameter	Value	Units	Ref
Sheave distance behind ship CG (*x*-axis)	62	m	[13]
Sheave distance beside ship CG (*y*-axis)	0	m	[7]
Sheave height above ship CG (*z*-axis)	8.2	m	[13]
Towed-body mass	1734	kg	[12]
Towed-body radius	0.45	m	[12]
Towline length	460	m	[7]
Towline drag coefficient	1.8		[7]
Towline axial stiffness	1.141	MN/m	[7]
Towline radius	0.0206	m	[7]
Towline density	3920	kg/m^3	[7]
Nominal tow speed	3.66	m/s	[13]

Preprint

Sun *et al.* [7], Zhu *et al.* [16], Hover *et al.* [17], Howell [18], and Driscoll *et al.* [19] describe and justify the assumption that tensile cable strain (describing the axial motion from tow-cable elongation) dominates curvature strain (describing the rotational motion from tow-cable bending) in full-scale high-tension towed applications. As a result, rotational stiffness and damping can be neglected for the full-scale simulator, and axial stiffness is included instead.

V. RESULTS

Results of the experimental tests are assessed by fitting an ellipsoid around the motion envelope of the spherical tow body such that sphere's position is contained within the ellipsoid 95% of the time. The ellipsoid volume is then used to assess the performance of the reference-point algorithm which was used for motion compensation such that the smaller the volume, the better the motion compensation. Fig. 10 illustrates a general ellipsoid with semi-principal axes X_E, Y_E, and Z_E and corresponding radii r_X, r_Y and r_Z, which are used to assess the new proposed reference-point algorithms described in Section II.

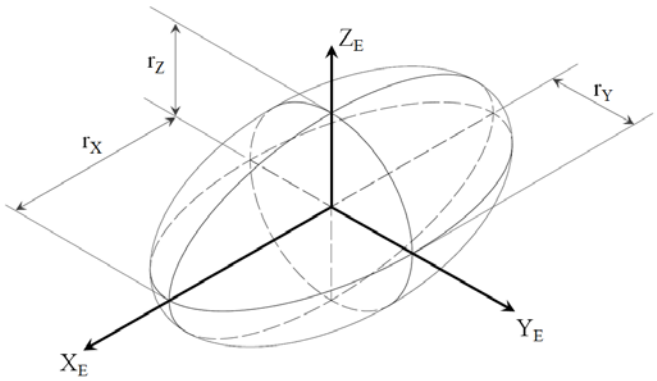

Fig. 10: Ellipsoid with semi-principle axes and radii identified.

To fit an ellipsoid to the spherical tow-body's motion envelope, first the origin of the ellipsoid reference frame shown in Fig. 10 is positioned on the centroid of the spherical tow-body's trace. The ellipsoid's X_E-axis is then oriented so that it is collinear with a best-fit line through the sphere's trace. Next, the plane formed by the ellipsoid's X_E and Y_E axes are oriented so that they are coplanar with a best-fit plane through the sphere's trace. The relative proportionality of the ellipsoid radii is then determined from the variance of the spherical tow-body's trace in the X_E, Y_E, and Z_E directions. A cost-minimization algorithm is ultimately used to scale the size of the ellipsoid such that 95% of the spherical tow-body's trace is contained within the bounds of the ellipsoid surface. Because each point along the trace is taken at a consistent time interval of 0.2 seconds, the result of the fitting process indicates that the towed sphere is located within the ellipsoid 95% of the time during the two-minute trial. Fig. 11 shows a sample towed-sphere motion trace with an ellipsoid fit for a flume tank test with no acting motion compensation mechanism.

Preprint

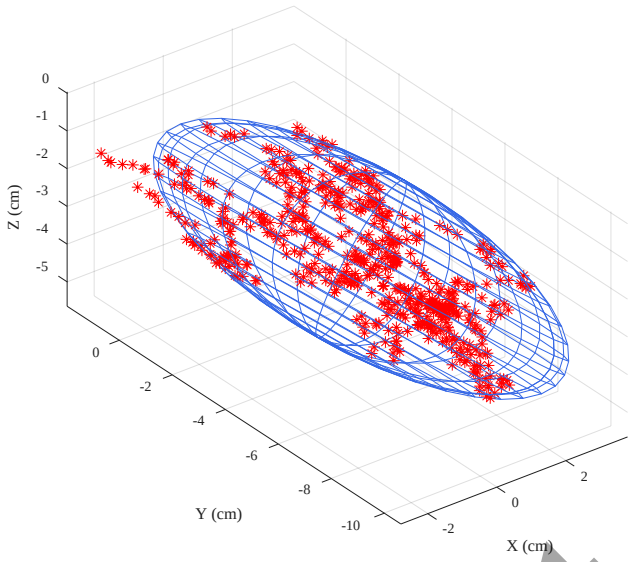

Fig. 11: Ellipsoid fit around towed-sphere trace for uncompensated motion trial.

A. Flume-scale simulation

To analyze the flume-tank test results, the experimental and simulated systems were first compared using two baseline trials, after which the performance of the proposed reference-point algorithms in the closed-loop motion compensation system was studied. The first baseline trial involved recording the towed sphere's trace in the fluid flow, but without any induced motion from the test mechanism. The resulting ellipsoid for a stationary mechanism case captured the effects of the flume tank turbulence on the submerged sphere and represented the smallest possible ellipsoid volume of 4.82 cm^3 achievable. This ellipsoid volume represents what the proposed reference-point algorithms should strive to achieve.

The second baseline trial involved moving the flume-scale test mechanism to follow the vertical and horizontal motions shown in Fig. 8 with no active motion compensation – a worst-case uncompensated system. The resulting ellipsoid for an uncompensated case represents the largest possible ellipsoid area, assuming that all reference-point algorithms offer some level of compensation. The baseline value for the uncompensated ellipsoid volume was 182.7 cm^3. These best- and worst-case baseline trials are used to provide a metric for comparing the four reference-point algorithms being tested.

Fig. 12 compares the resulting ellipsoid volumes of the different test cases under both experimental and simulated flume-scale conditions. It should be noted that the Rigorous Waterline case is absent from the figure, as it presented stability issues in both experimental and simulated trials. This algorithm was found to produce large responses to small changes in the sheave angle. For example, with the winch in its nominal position 46 cm above the waterline, an error of 1° in towline angle measurement in its expected

Preprint

range corresponds to an error of approximately 1 cm in towline length. The Rigorous Sheave algorithm was more robust in response to sensor error, since the algorithm calculates the control-loop reference signal based on the winch location, not on the difference in towline length above water. For the same error of 1º in sheave-angle measurement near its nominal range, the maximum expected error for the Rigorous Sheave method is approximately 0.13 mm.

Focusing on the experimental results presented in Fig. 12, as expected the uncompensated case demonstrates the largest amount of towed sphere motion, while the stationary mechanism case demonstrates the smallest amount of sphere motion. Amongst the proposed reference-point algorithms, the Rigorous Sheave algorithm performs better in the experiments than both the Simplified Sheave and Simplified Waterline algorithms. The Rigorous Sheave algorithm reduces motion in the experiments by 86% compared to the uncompensated case. The two Simplified algorithms perform nearly identically, reducing sphere motion by 80% compared to the uncompensated case.

Fig. 12 also indicates that the simulated ellipsoid volumes are consistently smaller than the experimental results. For all the test cases, simulated ellipsoid volume is approximately half of the experimental results. The reason for this difference is likely related to the simplification of turbulence effects and un-modelled fluid flow, tow-body and cable interactions within the simulation. The simulation trends, however, are consistent with the experimental results.

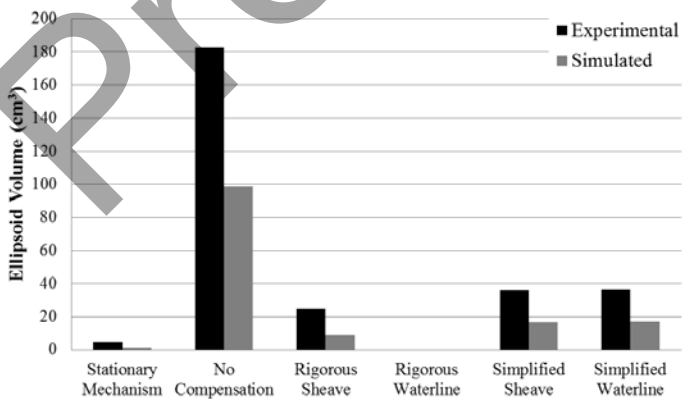

Fig. 12: Ellipsoid volume for experimental and simulated flume-scale results

Preprint

Fig. 13 summarizes the simulated and experimental test cases in terms of percent ellipsoid volume reduction relative to the uncompensated worst-case volume. Again, the Rigorous Waterline method is absent from this figure as it exhibited stability issues in both experiment and simulation.

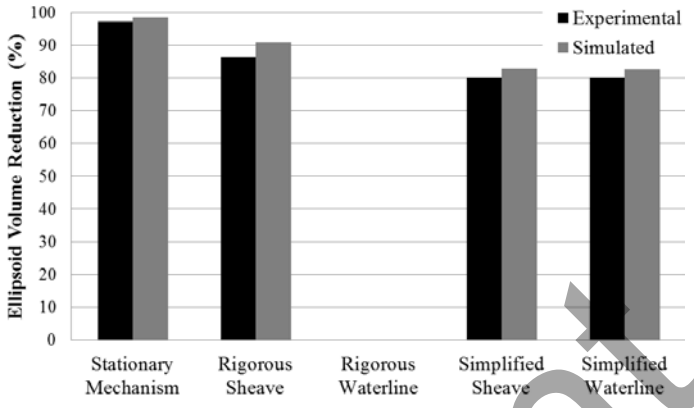

Fig. 13: Ellipsoid volume reduction relative to uncompensated case for experimental and simulated flume-scale results.

Fig. 13 indicates that the simulated ellipsoid volume reduction relative to the uncompensated case agrees well with the experimental results over all of the test cases. Using the simulator, the Rigorous Sheave algorithm performed the best reducing towed-body motion by 90%.

The results in Fig. 12 and Fig. 13 also show that the performance of the Simplified Sheave and Simplified Waterline algorithms are very similar. This similarity is a result of the geometry of the flume-scale setup; specifically, the nominal winch height, motion envelope, and length of tow cable. To observe a larger difference between the Simplified Sheave and Simplified Waterline methods, one would need to lower the nominal sheave height above the waterline, increase the size of the motion envelope, or increase the length of the tow cable. Due to space constraints and limitations of the flume-scale test environment, such changes could not be realized experimentally. As a result, the sheave height was lowered within the flume-scale simulator and the different cases were re-simulated.

B. Alternative geometry of flume-scale simulation

To investigate the influence of the position of the sheave height above the waterline on the different test cases, the nominal sheave height was lowered within the flume-scale simulator from 46 cm to 17 cm – a geometry which more accurately replicates a full-scale towed system aboard, for example, the FFG-7 vessel mentioned in the Australian DSTO report [13].

Preprint

In addition to altering the geometry of the test environment within the simulator, additional disturbances on the towed system were removed to simplify the analysis of the towed system as much as possible. In particular, the winch dynamics and PD controller were removed from the simulator so that the prismatic joint's position (which is used by the simulator to mimic the winch reeling cable in or out) was directly prescribed. Additionally, turbulence was removed from the simulator and the flow profile was simplified to a constant flow speed over all depths. Fig. 14 presents the results of the alternative-geometry flume-scale simulation environment.

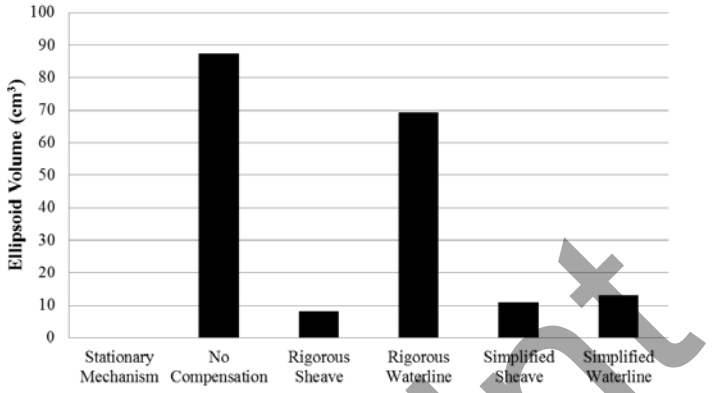

Fig. 14: Ellipsoid volume for the alternative-geometry simulated flume-scale results.

In the alternative-geometry simulation, the best case (Stationary Mechanism) had an ellipsoid volume of 0.0 cm^3 as expected since the sheave tow point was stationary and there were no fluid disturbances acting on the submerged body. The worst case (No Compensation) had an ellipsoid volume of 87.3 cm^3. The Rigorous Sheave reference-point algorithm still performed the best in the alternative geometry simulation, reducing ellipsoid volume by 91% compared to the uncompensated case. The relative difference between the Rigorous Sheave and the Simplified Sheave methods was less. The original geometry produced an improvement of 7% by applying the Rigorous formulation of the Sheave algorithm, while the alternative geometry reduced this improvement to only 3%. This reduction in performance in the alternative-geometry flume-scale simulations indicates that the apparent benefit of real-time sheave angle measurement shown in Figs. 12 and 13 might not be as significant in full-scale situations.

As expected, Fig. 14 shows a more noticeable difference between the Simplified Sheave algorithm and the Simplified Waterline algorithm than the previous results shown in Fig. 12 and Fig. 13. The Simplified Sheave algorithm reduced the ellipsoid volume by 88% compared to the uncompensated motion case, and the Simplified Waterline algorithm reduced the ellipsoid volume by 85% compared to the uncompensated motion case. The 3% difference between the two Simplified algorithms indicate that the Simplified Sheave algorithm might perform better than the Simplified Waterline algorithm in full-scale applications; however, this 3% difference might be difficult to measure or negligible in physical marine systems.

Preprint

It is interesting to note that, for the alternative geometry, the Rigorous Waterline algorithm remained partially stable throughout the alternative-geometry flume-scale simulation, but small changes in sheave angle still provoked large reference-point responses. Despite the erratic behaviour of the Rigorous Waterline algorithm, it was still able to reduce ellipsoid volume by 21% compared to the uncompensated motion case.

C. Full-scale simulation test cases

It is desirable to simulate the performance of the reference-point algorithms over a range of towed system parameters at full scale to obtain a more general sense of the relative performance of the algorithms.

The test cases presented in Table 6 provide a range of different tow-cable profiles under the waterline as illustrated in Fig. 15. The horizontal and vertical axes in Fig. 15 correspond to displacement from the host vessel's centre of gravity along the *x*- and *z*-directions, respectively. For the tow cables presented in Fig. 15, no ship disturbance is applied in simulation, so that the tow cables assume their steady-state curvature.

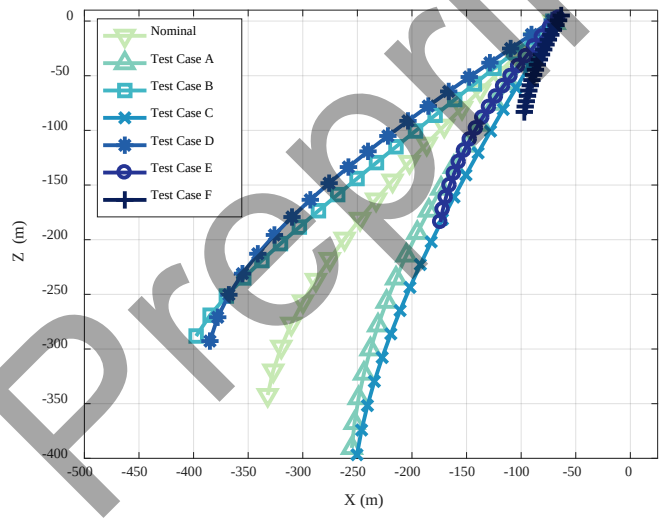

Fig. 15: Steady-state tow cable profiles for all full-scale test cases.

Test cases A and C have roughly similar tow-cable profiles, resulting from an increase in towed-body mass (case A) and a decrease in tow-cable drag (case C). Test cases B and D also have somewhat similar tow-cable profiles, resulting from a decrease in towed-body mass (case B) and an increase in tow-cable drag (case D). Test cases E and F demonstrate the effect of reducing the length of the towline.

Preprint

Fig. 16 shows a plot comparing the resulting ellipsoid volumes for the uncompensated and reference-point algorithms for each of the test cases outlined in Table 6. It should be noted that the test cases presented in Fig. 16 do not include the performance of the Rigorous Sheave algorithm since this algorithm demonstrated instabilities in the full-scale simulation.

TABLE 6: SUMMARY OF FULL-SCALE TEST CASE PARAMETERS

	Test Case						
Parameter	**Nominal**	**A**	**B**	**C**	**D**	**E**	**F**
Towline length	460 m	460 m	460 m	460 m	460 m	230 m	100 m
Towed-body mass	1734 kg	3468 kg	867 kg	1734 kg	1734 kg	1734 kg	1734 kg
Towline C_d	1.8	1.8	1.8	0.9	2.7	1.8	1.8

As with the flume-scale simulation, the Rigorous Sheave algorithm performed the best for all test cases, while the Simplified Waterline reference-point algorithm performed worse than both Sheave algorithms.

The Waterline algorithms assume that it is possible to maintain steady-state behaviour for the entire submerged towed system by ensuring that the same location on the tow cable crosses the waterline at all times. Theoretically, this method would, therefore, require a tow-cable discontinuity when it crosses the waterline as shown in Fig. 17. It is likely for this reason that the Simplified and Rigorous Sheave algorithms (which do not impose any discontinuity assumption on the tow cable) generally appear to be more effective at reducing towed-body motion than the Simplified and Rigorous Waterline algorithms.

Fig. 16 indicates that as tow cable length decreases (cases E and F), the performance of the Simplified Waterline algorithm improves and eventually approaches the performance of the Simplified Sheave algorithm. For the nominal case, the ellipsoid volume of the Simplified Waterline algorithm is 14 times larger than the ellipsoid volume of the Simplified Sheave algorithm. This ratio is reduced to approximately 4.5 for the 100 m tow cable in test case F. This trend linking tow-cable length and similarity between Simplified Sheave and Simplified Waterline algorithms agrees with results from flume-scale experimental and simulation work, which also showed similar performance of the Simplified Waterline and Simplified Sheave algorithms for a shallow tow.

Throughout the full-scale tests shown in Fig. 16, the performance of the Simplified Sheave algorithm was nearly identical to that of the Rigorous Sheave algorithm. The performance of the Simplified Sheave algorithm depends on the validity of the assumption that the sheave angle is a constant, nominal value. Sheave angle variation during full-scale simulations was found to be smaller than the flume-scale tests (which did show a difference between the Simplified and Rigorous Sheave algorithms). The standard deviation of the sheave angle was 0.9 degrees over the course of the nominal test case at full scale, while the standard deviation was 2.7 degrees in the flume-scale tests. It is likely this that reduction in sheave angle variation at full scale enabled the Simplified Sheave algorithm to perform better at full scale.

Preprint

Consistently good performance of the Simplified Sheave algorithm raises a question regarding the robustness of this approach when the nominal sheave angle on which it depends is assigned incorrectly. Full-scale simulations were, therefore, carried out for a range of assumed nominal sheave angles in order to further assess this method.

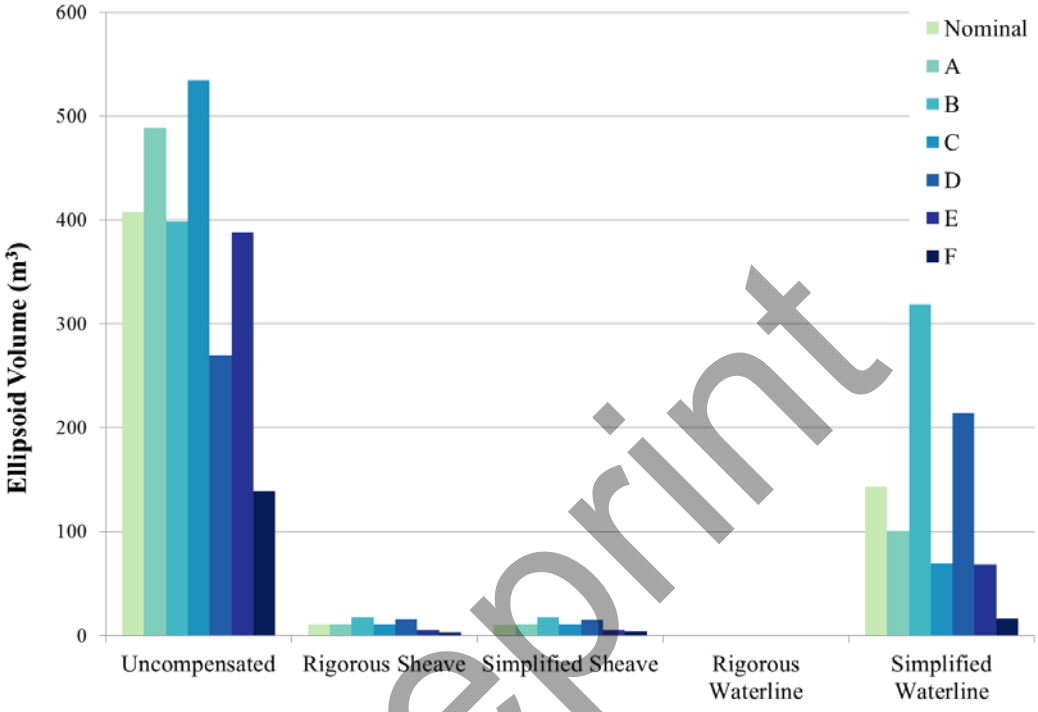

Fig. 16: Comparison of reference-point algorithms for various test cases at full scale.

Preprint

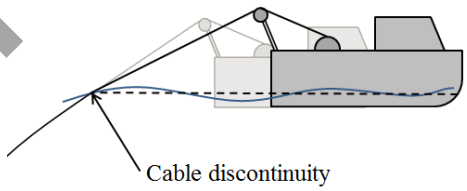

Fig. 17: Cable discontinuity required for proper implementation of Waterline reference-point algorithm.

Fig. 18 shows the resulting performance of the Simplified Sheave reference-point algorithm by plotting the ellipsoid volume for different assumed sheave angles. Note that the nominal sheave angle in Fig. 18 corresponds to 48 degrees which was used to generate the Simplified Sheave results shown in Fig. 16. The ellipsoid volume for the uncompensated case is also included in Fig. 18 to demonstrate the relative performance of the Simplified Sheave algorithm for the range of nominal sheave angles tested.

Fig. 18 shows that reasonable performance of the Simplified Sheave algorithm is maintained despite the presence of relatively large nominal sheave-angle errors used in the simulation. Although the introduction of 20 degrees of sheave-angle error into the reference-point algorithm increases the ellipsoid volume by a factor of 5 over the nominal case, the resulting performance is still very good (with an ellipsoid reduction relative to the uncompensated case of 87% to 89%). The robustness of this method suggests that, for the conditions used in this research, it may be possible to use the Simplified Sheave algorithm for motion compensation even when a rough estimate of sheave angle is used.

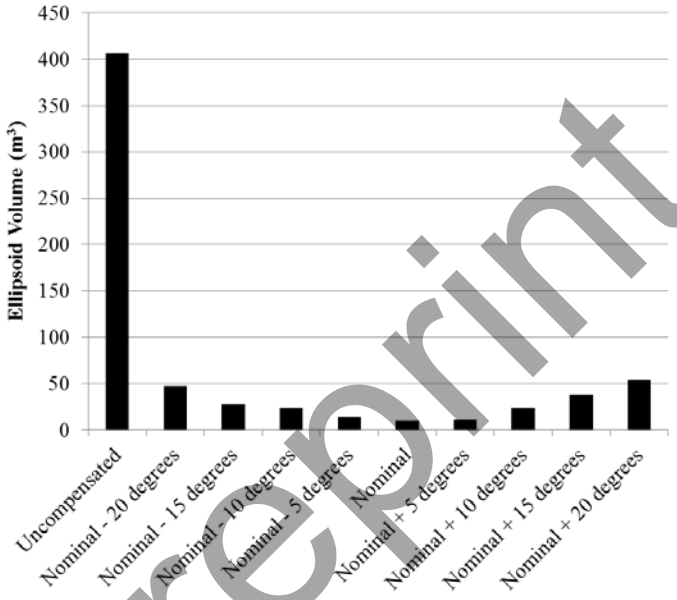

Fig. 18: Performance of Simplified Sheave algorithm with nominal sheave error.

VI. Conculsions and Future Work

Of the four reference-point compensation methods which were explored in this paper, for the conditions used in this research the Rigorous and Simplified Sheave algorithms generally proved to be most effective in both simulation and experimentation. While the Rigorous Sheave algorithm outperformed the Simplified Sheave algorithm in the flume-scale simulation and experimental results, their performance was nearly identical in the full-scale simulations. Additionally, the Simplified Sheave algorithm demonstrates robustness to nominal sheave angle error, indicating a potential cost-saving opportunity through the reduction of real-time sheave-angle measurements.

It is suggested that full-scale experiments and simulations be carried out with realistic towed-body geometries so that a more complete understanding of the performance of these reference-point algorithms at full-scale can be achieved.

Preprint

ACKNOWLEDGMENTS

The authors would like to thank Natural Sciences and Engineering Research Council of Canada (NSERC), Carleton University and Dalhousie University for their financial support of this research. The authors would also like to thank Rolls-Royce Canada Limited for their in-kind support of the work.

REFERENCES

[1] J. K. Woodacre, R. J. Bauer and R. A. Irani, "A review of vertical motion heave compensation systems," *Ocean Engineering,* vol. 104, pp. 140-154, 2015.

[2] B. Yang, K. Zhu and D. Qin, "Dynamic response of towed line array," *Journal of Hydrodynamics,* vol. 25, no. 4, pp. 616-619, 2013.

[3] J. Kamman and R. Huston, "Multibody dynamics modeling of variable length cable systems," *Multibody System Dynamics,* vol. 5, no. 3, pp. 211-221, 2001.

[4] F. Wang, G. Huang and D. Deng, "Steady state analysis of towed marine cables," *Journal of Shanghai Jiaotong University (Science),* vol. 13, no. 2, pp. 239-244, 2008.

[5] C. Lambert, M. Nahon, B. Buckham and M. Seto, "Dynamics and control of a towed underwater vehicle system, part I: model development," *Ocean Engineering,* vol. 30, no. 4, pp. 453-470, 2003.

[6] R. Driscoll and M. Nahon, "Mathematical modeling and simulation of a moored buoy system," in *Oceans Conference Record (IEEE)*, Fort Lauderdale, Florida, 1996.

[7] F. Sun, Z. H. Zhu and M. Larosa, "Dynamics modeling of cable towed body using nodal position finite element method," *Ocean Engineering,* vol. 38, no. 4, pp. 529-540, 2011.

[8] H. I. Park, D. H. Jung and W. Koterayama, "A numerical and experimental study on dynamics of a towed low tension cable," *Applied Ocean Research,* vol. 25, no. 5, pp. 289-299, 2003.

[9] C. Calnan, R. Bauer and R. Irani, "Controller design and motion compensation for marine towed bodies," in *Oceans 2016 MTS/IEEE*, Monterey, California, 2016.

[10] Nortek Instruments, "Vectrino high-resolution acoustic doppler velocimeter," datasheet.

Preprint

[11] W. Quan, Y. Liu, Z. Zhang, X. Li and C. Liu, "Scale model test of a semi-active heave compensation system for deep-sea tethered ROVs," *Ocean Engineering*, vol. 126, pp. 353-363, 2016.

[12] C. O. Walton and R. E. Billhart, "The stability derivatives of the scheme a body uses with the AN/SQA-13 (XN-1) variable depth sonar system," Hydromechanics Laboratory David Taylor Model Basin Department of the Navy, 1966.

[13] A. M. Arney, "FFG-7 ship motion and airwake trial. Part II: removal of ship motion effects from measured airwake data," Air Operations Division Aeronautical and Maritime Research Laboratory, Melbourne Victoria, Australia, 1994.

[14] R. Irani, R. J. Bauer, L. North, M. Nicholson, D. Nolan and B. West, "Analysis of joint failures on the lateral undulation gait of a robotic snake," *Transactions of the Canadian Society for Mechanical Engineering*, vol. 39, no. 2, pp. 253-268, 2015.

[15] C. Calnan, "Set-point algorithms for active heave compensation of towed bodies," Master's Thesis, Dalhousie University, Canada, 2016.

[16] Z. Zhu, S. Meguid and L. Ong, "Dynamic multiscale simulation of towed cable and body," in *Computational Fluid and Solid Mechanics*, 2003, pp. 800-803.

[17] F. Hover, M. Grosenbaugh and M. Triantafyllou, "Calculation of dynamic motions and tensions in towed underwater cables," *IEEE Journal of Oceanic Engineering*, vol. 19, no. 3, pp. 449-457, 1994.

[18] C. Howell, "Investigation of the dynamics of low-tension cables," Ph.D. Thesis, Massachusetts Institute of Technology, United States, 1992.

[19] F. R. Driscoll, R. G. Lueck and M. Nahon, "Development and validation of a lumped-mass dynamics model of a deep-sea ROV system," *Applied Ocean Research*, vol. 22, no. 3, pp. 169-182, 2000.

Preprint